

## RESEARCH ARTICLE

# Stress-activated MAPKs and CRM1 regulate the subcellular localization of Net1A to control cell motility and invasion

Arzu Ulu<sup>1</sup>, Wonkyung Oh<sup>2</sup>, Yan Zuo<sup>1</sup> and Jeffrey A. Frost<sup>1,\*</sup>

## ABSTRACT

The neuroepithelial cell transforming gene 1A (Net1A, an isoform of Net1) is a RhoA subfamily guanine nucleotide exchange factor (GEF) that localizes to the nucleus in the absence of stimulation, preventing it from activating RhoA. Once relocalized in the cytosol, Net1A stimulates cell motility and extracellular matrix invasion. In the present work, we investigated mechanisms responsible for the cytosolic relocalization of Net1A. We demonstrate that inhibition of MAPK pathways blocks Net1A relocalization, with cells being most sensitive to JNK pathway inhibition. Moreover, activation of the JNK or p38 MAPK family pathway is sufficient to elicit Net1A cytosolic localization. Net1A relocalization stimulated by EGF or JNK activation requires nuclear export mediated by CRM1. JNK1 (also known as MAPK8) phosphorylates Net1A on serine 52, and alanine substitution at this site prevents Net1A relocalization caused by EGF or JNK activation. Glutamic acid substitution at this site is sufficient for Net1A relocalization and results in elevated RhoA signaling to stimulate myosin light chain 2 (MLC2, also known as MYL2) phosphorylation and F-actin accumulation. Net1A S52E expression stimulates cell motility, enables Matrigel invasion and promotes invadopodia formation. These data highlight a novel mechanism for controlling the subcellular localization of Net1A to regulate RhoA activation, cell motility, and invasion.

**KEY WORDS:** Net1A, RhoA, Breast cancer metastasis, JNK, MAPK, CRM1

## INTRODUCTION

Rho GTPases are fundamental regulators of actin cytoskeletal organization, cell motility and cancer metastasis (Heasman and Ridley, 2008; Jaffe and Hall, 2005). In the cell, they function as molecular switches, cycling between their active, GTP-bound, and inactive, GDP-bound, states. When active, Rho proteins interact with effector proteins that mediate downstream signaling (Bishop and Hall, 2000). Rho GTPase activation is controlled by a family of proteins known as guanine nucleotide exchange factors (GEFs), which stimulate GDP release to allow GTP binding (Rossman et al., 2005). The neuroepithelial cell transforming gene 1 (Net1) is a RhoA- and RhoB-specific GEF that is overexpressed in a number of human cancers, including breast cancer (Bennett et al., 2011; Dutertre et al., 2010; Murray et al., 2008; Shen et al., 2008; Tu et al., 2010). We have shown that co-expression of Net1 and  $\beta 4$  integrin is

prognostic for decreased distant metastasis-free survival in estrogen receptor positive breast cancer patients (Gilcrease et al., 2009). Consistent with this, we have found that the Net1A isoform of Net1 regulates breast cancer cell motility and invasive capacity *in vitro* (Carr et al., 2013a; Song et al., 2015).

Net1 isoforms are unusual among RhoGEFs in that they localize to the nucleus in quiescent cells, thereby preventing them from accessing RhoA present at the plasma membrane (Qin et al., 2005; Schmidt and Hall, 2002). Two isoforms of Net1 exist in most cells, Net1 and Net1A, which differ in their N-terminal regulatory domains. Importantly, stimulation of cells by integrin engagement or treatment with ligands such as epidermal growth factor (EGF) promotes cytosolic accumulation of the Net1A isoform. Moreover, the ability of EGF to cause Net1A cytosolic localization is entirely dependent on Rac1 activation (Song et al., 2015). Importantly, these stimuli do not cause cytosolic accumulation of the longer Net1 isoform, consistent with the requirement for Net1A, but not Net1, for cell adhesion and motility (Carr et al., 2013a,b).

Owing to the critical role of subcellular localization in controlling Net1A activity, identifying mechanisms regulating the cytosolic accumulation of Net1A is essential to understanding how it drives RhoA activation and cell motility. Previously, we have shown that cytosolic localization of Net1A following integrin ligation is dependent upon Rac1 activation and limited by proteasome-mediated degradation (Carr et al., 2013a). Additionally, cytosolic accumulation of Net1A following EGF stimulation depends upon Rac1 and is extended by acetylation near the second of its two nuclear localization sequences (NLSs), which slows the rate of nuclear re-import (Song et al., 2015). However, these mechanisms only partially account for how Net1A cytosolic localization is controlled, since they do not explain how Rac1 activation signals to Net1A to control its cytosolic accumulation. Similarly, they do not explain the mechanism by which nuclear exit of Net1A is achieved.

To determine how Rac1 signals to Net1A, we considered effector pathways that had the potential to interact with nuclear pools of Net1A. Top among these were the ERK, JNK and p38 MAPK family pathways, since they are all regulated by Rac1, and the MAPKs themselves are well known to move from the cytosol to the nucleus upon activation (Bishop and Hall, 2000; Cuadrado and Nebreda, 2010; Raman et al., 2007; Weston and Davis, 2007). Moreover, previous work has shown that MAPK pathways can contribute to cell motility through the phosphorylation of numerous cytosolic and nuclear substrates (Ebelt et al., 2013; Sever and Brugge, 2015; Wagner and Nebreda, 2009). Net1 has also been implicated in controlling JNK pathway activation, in that expression of a constitutively cytosolic Net1 truncation mutant, Net1 $\Delta$ N, stimulates JNK activation through an MKK7 (also known as MAP2K7)- and CNK1 (also known as CNKSR1)-dependent pathway (Alberts and Treisman, 1998; Jaffe et al., 2004, 2005).

In the present work, we demonstrate that small-molecule-mediated inhibition of each of the three MAPK families prevents

<sup>1</sup>Department of Integrative Biology and Pharmacology, University of Texas Health Science Center at Houston, Houston, TX 77030, USA. <sup>2</sup>DNA Repair Research Center, Chosun University, Gwangju 61452, Republic of Korea.

\*Author for correspondence (Jeffrey.a.frost@uth.tmc.edu)

© J.A.F., 0000-0001-9722-1536

cytosolic localization of Net1A following EGF stimulation, although cells appear to be most sensitive to inhibition of the JNK pathway. Activation of the JNK or p38 MAPK pathways in the absence of EGF stimulation is sufficient for Net1A cytosolic relocalization. Both EGF and active MKK7 require the nuclear exportin CRM1 to promote Net1A cytosolic localization. We also find that JNK1 (also known as MAPK8) phosphorylates Net1A on serine 52, and that this is required for cytosolic localization of Net1A following EGF stimulation. Moreover, acidic substitution of the JNK1 phosphorylation site is sufficient for Net1A cytosolic localization, RhoA activation and actin cytoskeletal reorganization. In addition, Net1A S52E expression stimulates cell motility, enables Matrigel invasion and promotes invadopodia formation. These data demonstrate a mechanistic link between JNK signaling and the RhoGEF Net1A to control RhoA activation, cell motility and invasion.

## RESULTS

### Multiple MAPK pathways regulate Net1A cytosolic relocalization

Previously, we have shown that ligands such as EGF stimulate Net1A relocalization from the nucleus to the cytosol in a Rac1-dependent manner (Carr et al., 2013a; Song et al., 2015). To better understand how EGF-stimulated Rac1 activation controls Net1A relocalization, we considered key cell signaling pathways regulated by Rac1 (Bishop and Hall, 2000). One family of signaling pathways we thought to be particularly likely to control Net1A localization were the ERK, JNK and p38 MAPK pathways. This was due to the ability of proteins involved in these pathways to translocate into the nucleus upon activation, and the demonstrated roles of these pathways in controlling cell motility (Ebelt et al., 2013; Sever and Brugge, 2015; Wagner and Nebreda, 2009).

To assess their roles in regulating Net1A localization, we tested the ability of small-molecule inhibitors of each MAPK pathway to prevent cytosolic localization of Net1A after EGF stimulation. EGF is best known as an activator of the ERK1 and ERK2 (ERK1/2; also known as MAPK3 and MAPK1, respectively) pathway, but it also stimulates the JNK and p38 MAPK pathways, albeit more weakly (Johnstone et al., 2005; Xia et al., 1995). MCF7 cells were transfected with HA–Net1A, serum-starved, and then pretreated with the inhibitors of JNK1 and JNK2 (JNK1/2; JNK2 is also known as MAPK9), p38 $\alpha$ , p38 $\beta$  and p38 $\gamma$  (also known as MAPK14, MAPK11 and MAPK12, respectively), or MEK1 and MEK2 (MEK1/2; also known as MAP2K1 and MAP2K2, respectively) for half an hour. The cells were transfected with HA–Net1A because antibodies suitable for detection of the endogenous Net1A isoform by immunofluorescence are not available. Cells were then stimulated with EGF for 15 min, which is the peak time for ligand stimulated cytosolic localization of Net1A (Song et al., 2015). The cells were then fixed and stained for HA–Net1A localization, F-actin and DNA (Fig. 1A,B). Net1A localization in each cell was assessed by performing epifluorescence microscopy and quantified as the ratio of cytosolic to nuclear staining. We have shown previously that assessing Net1A localization in this manner takes into account the inherent variation in transgene expression in transiently transfected cells and is linear over a wide range of expression (Song et al., 2015). As expected, Net1A was primarily nuclear in serum-starved cells, and EGF stimulation increased the cytosolic-to-nuclear ratio of Net1A by 2- to 3-fold (Fig. 1C; lower magnification micrograph in Fig. S1). However, pre-incubation with the JNK1/2 inhibitor SP600125 (denoted JNKi) completely blocked Net1A cytosolic localization (Fig. 1A–C). Surprisingly, pre-treatment

with the p38 inhibitor SB202190 (p38i), or the MEK1/2 inhibitor U1026 (MEKi), also blocked Net1A relocalization, although they were less effective than the JNK inhibitor (Fig. 1D–G). The ability of each inhibitor to block its target enzymes was demonstrated by western blotting (Fig. S2). Moreover, each inhibitor was specific for its intended target and did not block activation of the other MAPK pathways (Fig. S3). These data indicate that all three MAPK pathways contribute to the cytosolic localization of Net1A after EGF stimulation, although cells are somewhat more sensitive to JNK pathway inhibition.

Since EGF is not a potent activator of JNK signaling, we also tested the effect of tumor necrosis factor  $\alpha$  (TNF $\alpha$ ; also known as TNF) stimulation on Net1A subcellular localization. TNF $\alpha$  primarily stimulates the JNK and p38 MAPK pathways (Kant et al., 2011; Roulston et al., 1998). We observed that treatment of MCF7 cells with TNF $\alpha$  for 30 min also potently stimulated Net1A cytosolic localization (Fig. 1H,I). Importantly, this effect was abrogated by pre-treatment with the JNK or p38 inhibitors, but was not affected by MEK1/2 inhibition. Western blotting showed that TNF $\alpha$  potently stimulated JNK activation, and was a less effective activator of the p38 and ERK1/2 MAPKs. In addition, each inhibitor blocked its intended target enzymes (Fig. S4). These data indicate that both EGF and TNF $\alpha$  require stress-activated MAPKs to stimulate Net1A cytosolic localization, and support the notion that inhibition of JNK signaling is the most effective means to block Net1A relocalization.

To assess whether stimulation of the stress activated JNK and p38 MAPK pathways was sufficient for Net1A relocalization, MCF7 cells were transfected with Net1A, plus or minus constitutively active MKK7 or MKK3 (also known as MAP2K3). MKK7 and MKK3 are specific activators of the JNK and p38 MAPKs, respectively (Enslen et al., 1998; Schaeffer and Weber, 1999; Tournier et al., 1999, 2001). In these experiments, cells were stained for active MKK proteins as well as Net1A, and only cells expressing both proteins were quantified. We observed that co-expression of active MKK7 or MKK3 caused cytosolic relocalization of Net1A in starved cells, which was equivalent to or greater than the effect of EGF (Fig. 2). Importantly, addition of EGF did not significantly increase Net1A relocalization in MKK7- or MKK3-transfected cells, indicating that they maximally stimulated Net1A relocalization (Fig. 2).

We have shown previously that Net1A is required for breast cancer cell motility and invasion (Carr et al., 2013b). To determine whether JNK signaling is required for Net1A cytosolic localization in invasive breast cancer cells, we evaluated the effects of JNK inhibition on Net1A relocalization in BT-20, MDA-MB-453 and MDA-MB-436 cells. Both BT-20 and MDA-MB-436 cells express EGFR, while MDA-MB-436 cells express HER2 (also known as ERBB2) (Holliday and Speirs, 2011; Rae et al., 2004; Subik et al., 2010). Cells were transfected with HA–Net1A, treated or not with JNK inhibitor, and then stimulated for 15 min with EGF (BT-20 and MDA-MB-436), heregulin (MDA-MB-453) or fetal bovine serum (FBS) (MDA-MB-436). As we observed for MCF7 cells, we found that Net1A cytosolic localization was acutely sensitive to ligand stimulation in each of these cell lines (Fig. 3A–D). Importantly, cytosolic localization of Net1A was completely blocked by pretreatment with SP600125 in all three of the invasive breast cancer cell lines. These data indicate that the requirement for JNK pathway activation for Net1A cytosolic localization extends to multiple invasive breast cancer cell lines, and suggest that JNK pathway regulation of Net1A cytosolic localization is a generalizable effect.

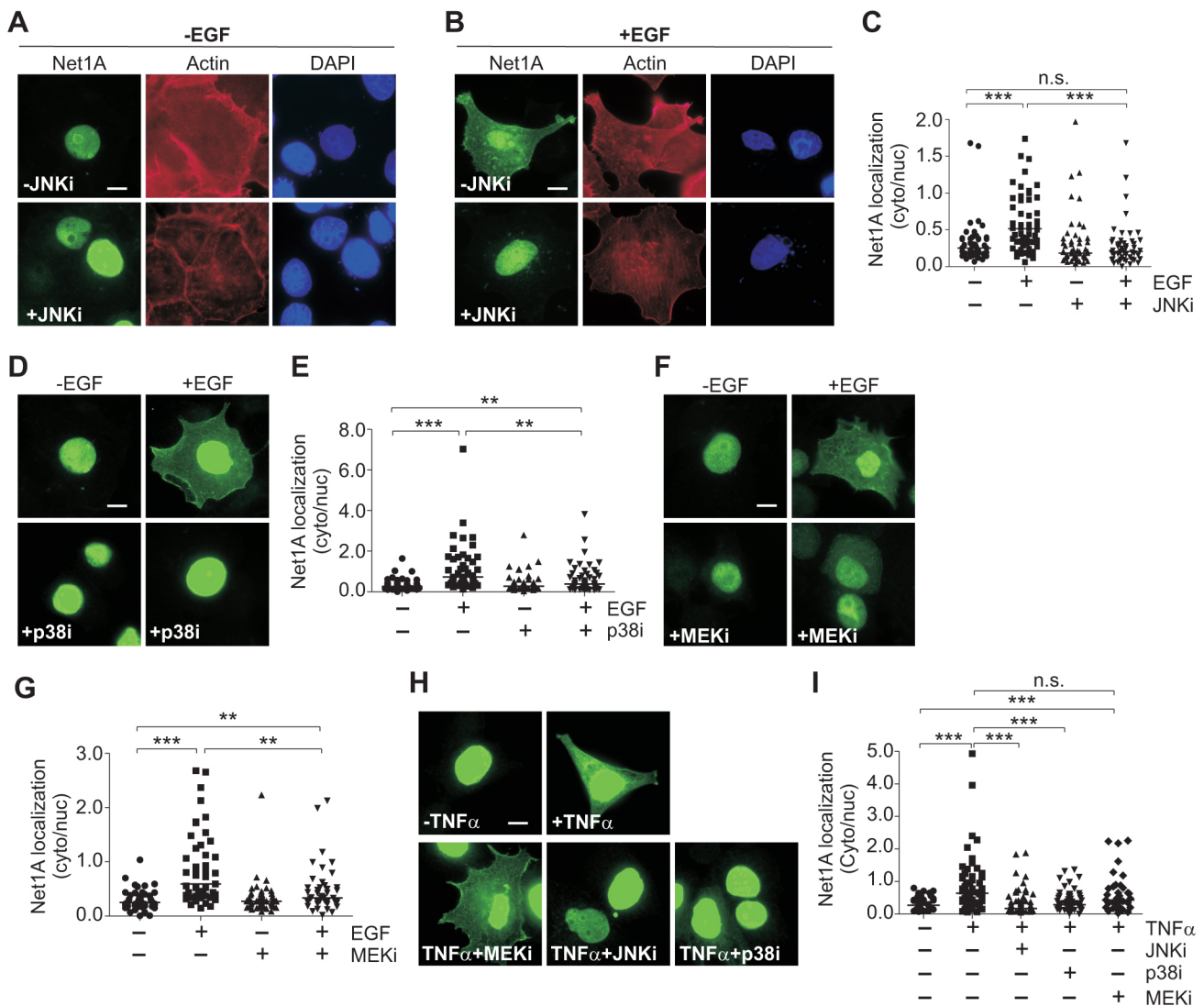


**Fig. 1. MAPK pathway inhibition blocks EGF- and TNF- $\alpha$ -induced Net1A cytosolic localization.** MCF7 cells expressing HA-Net1A were serum starved overnight, stimulated with EGF (100 ng/ml) for 15 min, fixed and stained for HA-Net1A localization. Prior to EGF stimulation, some cells were pretreated with the JNK inhibitor SP600125 (10  $\mu$ M; +JNKi) (A–C,H,I), the p38 inhibitor SB202190 (10  $\mu$ M; +p38i) (D,E,H,I), or the MEK inhibitor UO126 (10  $\mu$ M; +MEKi) (F,G,H,I) for 30 min. A, B, D, F and H show representative images of HA-Net1A staining. A and B include staining for F-actin (red) and DNA (blue). C, E, G and I show quantification of Net1A localization. Data were obtained from at least three independent experiments for EGF stimulation and two experiments for TNF $\alpha$ . For all experiments, at least 20 cells per condition were quantified. The line indicates the median value. \*\* $P$ <0.01; \*\*\* $P$ <0.001; n.s., not significant. Scale bars: 10  $\mu$ m.

### CRM1 is required for Net1A cytosolic relocalization

Previously, it has been shown that cytosolic localization of the Net1 N-terminal truncation mutant Net1 $\Delta$ N requires the activity of the nuclear exportin CRM1 (Schmidt and Hall, 2002). This mutant still contains one of the four NLS sequences present in full-length Net1 and thus exhibits partial nuclear localization (Song et al., 2015). To assess whether Net1A relocalization to the cytosol also requires CRM1, we treated cells with the CRM1 inhibitor leptomycin B (LMB) for 2 h prior to EGF stimulation. We observed that Net1A cytosolic localization was dependent upon CRM1 activity (Fig. 4A,B). To determine whether JNK-stimulated Net1A relocalization also required CRM1, cells were transfected with Net1A and active MKK7, and then treated with leptomycin B overnight. Importantly, CRM1 inhibition also blocked Net1A cytosolic localization caused by active MKK7 expression (Fig. 4C,D). Thus, EGF- and JNK-dependent Net1A relocalization to the cytosol requires active nuclear export by CRM1.

### JNK1 phosphorylation of Net1A on serine 52 is necessary for EGF-stimulated Net1A relocalization

Because JNK activity was required for EGF-stimulated relocalization of Net1A, we tested whether it could phosphorylate Net1A *in vitro*. For these assays, we used recombinant purified GST-Net1A and JNK1 to preclude the presence of other kinases or accessory proteins. We observed that GST-Net1A was efficiently phosphorylated by JNK1 *in vitro* (Fig. 5A). To identify the site(s) phosphorylated by JNK1, an *in vitro* kinase assay was repeated with GST-Net1A, JNK1 and unlabeled ATP, and phosphorylated peptides were identified by liquid chromatography tandem mass spectrometry (LC-MS/MS). This approach identified a number of phosphorylated Net1A peptides. However, a peptide containing phosphorylated serine 52 was the major phosphorylated species, as evidenced by the large number of peptides identified and the highest average ambiguity score for phosphorylation within these peptides (Ascore) (Fig. 5B). An Ascore reflects the likelihood of a particular

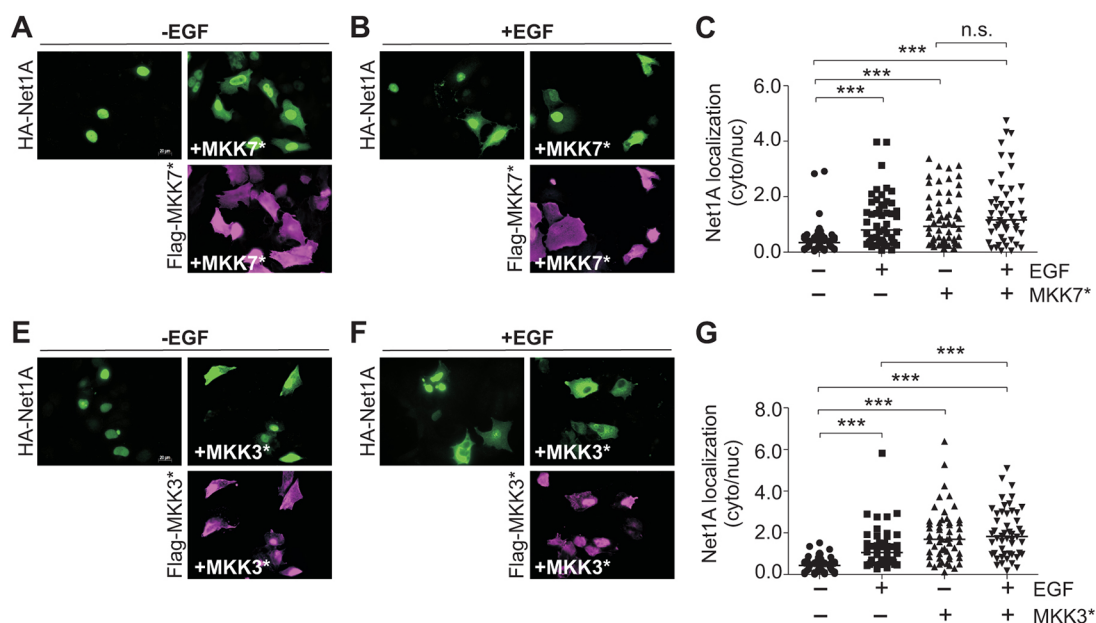


**Fig. 2. Effects of constitutively active MKK7 and MKK3 expression on Net1A cytosolic localization.** MCF7 cells were transfected with HA-Net1A with or without constitutively active Flag-MKK7\* (A–C) or Flag-MKK3\* (D–F) and starved overnight. After stimulation with EGF (15 min), cells were fixed and stained for HA-Net1A (green) and Flag-tagged MKKs (magenta). Representative images are shown. All data were obtained from at least three independent experiments. For all experiments, at least 20 cells per condition were quantified. The line indicates the median values. \*\*\* $P < 0.001$ ; n.s., not significant. Scale bars: 20  $\mu\text{m}$ .

residue being phosphorylated within a given peptide (Beausoleil et al., 2006). Interestingly, serine 52 is contained within a region between the two NLS sequences of Net1A (Fig. 5B) (Song et al.,

2015). To determine whether this site is required for Net1A cytosolic relocalization, we tested the effect of substitution of an alanine residue for serine 52 on EGF-stimulated Net1A

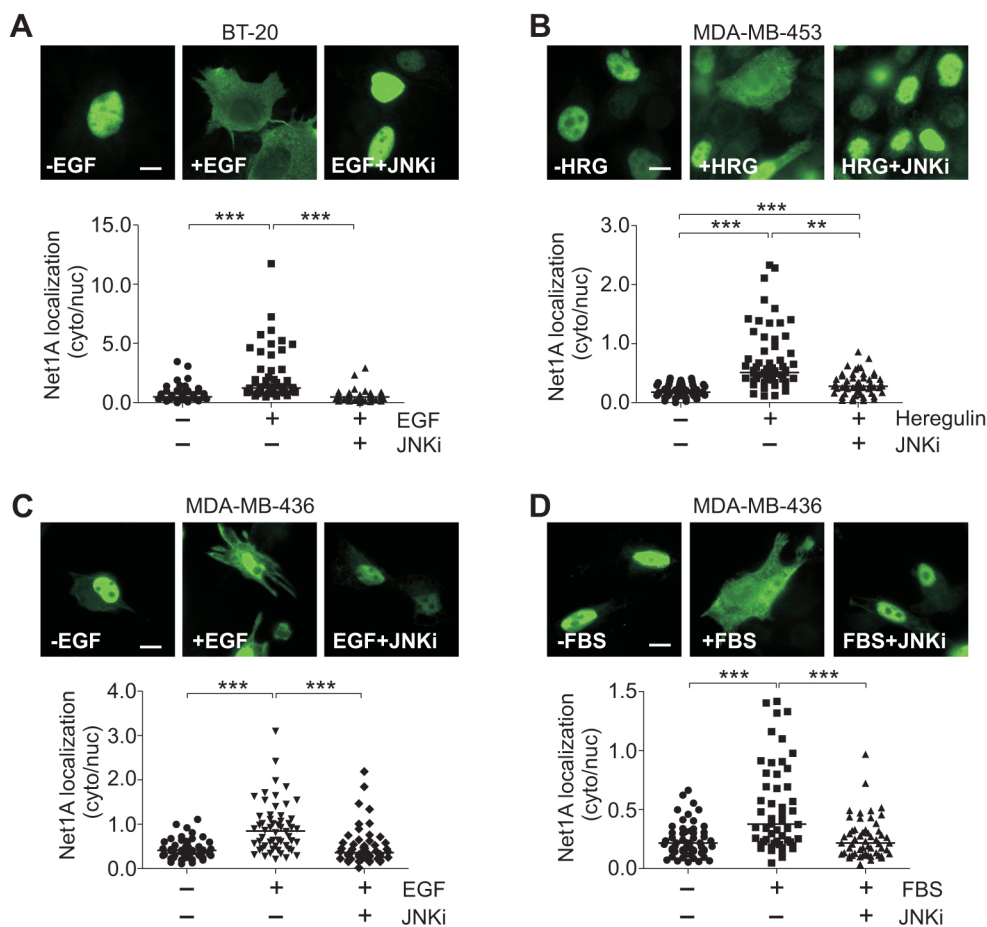


**Fig. 3. Cytosolic localization of Net1A is regulated by JNK in invasive human breast cancer cells.** BT-20 (A), MDA-MB-453 (B) and MDA-MB-436 (C,D) cells were transfected with HA-Net1A, serum starved overnight, and stimulated for 15 min with EGF (A,C), heregulin (HRG) (B) or 10% FBS (D). Where indicated cells were treated with 10  $\mu\text{M}$  SP600125 (+JNKi). Cells were fixed and stained for HA-Net1A localization. Representative images are shown. All data were obtained from three independent experiments. For all experiments, at least 20 cells per condition were quantified. The line indicates the median values. \*\* $P < 0.01$ ; \*\*\* $P < 0.001$ . Scale bars: 10  $\mu\text{m}$ .

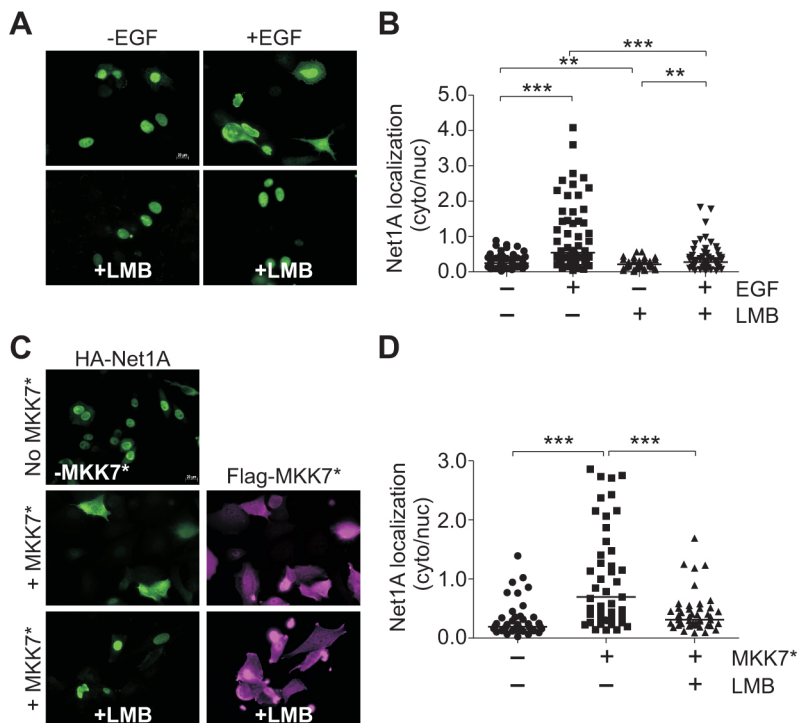


**Fig. 4. CRM1 is required for EGF- and MKK7-stimulated Net1A cytosolic relocalization.** (A,B) MCF7 cells were transfected with HA-Net1A, serum starved overnight, and then stimulated with EGF (15 min). In some cases cells were pretreated for 2 h with the CRM1 inhibitor leptomycin B (+LMB, 10  $\mu$ M). Cells were then fixed and stained for HA-Net1A. Representative images are shown. Data were obtained from three independent experiments. (C,D) MCF7 cells were transfected with HA-Net1A, with or without constitutively active Flag-MKK7\*. Cells were serum starved and treated with LMB overnight. Cells were then fixed and stained for HA-Net1A (green) and Flag-MKK7\* (magenta). Representative images are shown. Data were obtained from three independent experiments. For all experiments, at least 20 cells per condition were quantified. The line indicates the median values. \*\* $P$ <0.01; \*\*\* $P$ <0.001. Scale bars: 20  $\mu$ m.

relocalization. These experiments showed that Net1A cytosolic localization was completely dependent upon this site, as the S52A mutant failed to relocalize to the cytosol following EGF stimulation (Fig. 5C,D). This mutant also did not relocalize in cells co-transfected with constitutively active MKK7 (Fig. 5E,F). To determine whether phosphorylation of this site was sufficient for Net1A relocalization, we tested the effect of glutamate substitution of serine 52. We observed that Net1A S52E was constitutively localized to the cytosol in serum-starved cells, and that stimulation with EGF did not cause additional cytosolic localization (Fig. 6A,B). Cytosolic localization of Net1A S52E was also insensitive to treatment with the JNK inhibitor SP600125, indicating that JNK activity was no longer required (Fig. 6C,D). Overall, these results indicate that phosphorylation of serine 52 by JNK is necessary and sufficient for EGF-induced Net1A relocalization to the cytosol.

We have shown previously that Net1A residence in the cytosol is limited by proteasome-mediated degradation as well as its rate of nuclear re-import (Carr et al., 2009, 2013a; Song et al., 2015). Because serine 52 is located between the two NLS sequences of Net1A, we hypothesized that phosphorylation of this site might slow the rate of nuclear re-import. To determine whether this was the case, MCF7 cells were transfected with wild-type or S52E Net1A, and then treated with the nuclear importin  $\beta$  inhibitor importazole. Importazole blocks the interaction of importin  $\beta$  with NLS cargo proteins and importin  $\alpha$  subunits, thereby preventing nuclear import of NLS-containing proteins (Soderholm et al., 2011). We observed that importazole treatment caused a significant accumulation of wild-type Net1A in the cytosol in the absence of ligand stimulation, indicating that Net1A nuclear import was regulated by importin  $\beta$  (Fig. 6E, top panels; Fig. 6F). Importantly, importazole had little effect on the overall levels of Net1A S52E in the cytosol, suggesting that its localization was not regulated by importin  $\beta$  (Fig. 6E, control versus importazole; Fig. 6G). To measure the kinetics of Net1A nuclear re-import, the importazole was washed out and the cells were given different amounts of time for Net1A to traffic back into the nucleus. Concurrent with importazole washout, the cells were

treated with cyclohexamide to prevent new synthesis of Net1A, leptomycin B to prevent Net1A nuclear export, and MG132, to prevent proteasome-mediated degradation of Net1A. These added treatments were necessary to prevent confounding effects of each of these processes on Net1A localization. We observed that wild-type Net1A was efficiently re-imported into the nucleus under these conditions, such that cytosolic levels of Net1A reached control levels by 4 h (Fig. 6E,F). On the other hand, Net1A S52E localization in the cytosol was stable over the 8 h of the experiment, indicating that it was not significantly re-imported into the nucleus. These data suggest that phosphorylation of serine 52 causes Net1A accumulation in the cytosol by inhibiting its nuclear import, presumably by preventing interaction with one or more nuclear importins.

#### Cytosolic relocalization of Net1A stimulates RhoA signaling

Since Net1A is a RhoA-specific GEF, we tested whether expression of Net1A S52E stimulated RhoA signaling. Myosin light chain 2 (MLC2, also known as MYL2) phosphorylation and F-actin accumulation are well established RhoA signaling readouts, which we have shown previously to require Net1A expression in breast cancer cells (Carr et al., 2013b). Therefore, we assessed the effect of Net1A S52E expression on MLC2 phosphorylation and F-actin accumulation in serum-starved cells by means of immunofluorescence. We observed that cells transfected with Net1A S52E exhibited a strong increase in MLC2 phosphorylation and F-actin staining as compared to cells transfected with nuclear localized  $\beta$ -galactosidase ( $\beta$ -Gal) or wild-type Net1A (Fig. 7A–C).

To determine whether phosphorylation of serine 52 altered Net1A catalytic activity towards RhoA, we performed GST-A<sup>17</sup>RhoA pulldown assays. A<sup>17</sup>RhoA is a nucleotide-free version of RhoA that only interacts with active RhoA GEFs (Carr et al., 2013a; Garcia-Mata et al., 2007; Song et al., 2015). These assays showed that the activity of Net1A S52E was not appreciably different from that of wild-type Net1A. Similarly, the activation state of Net1A S52A was also comparable to that of wild-type Net1A (Fig. 7D,E).

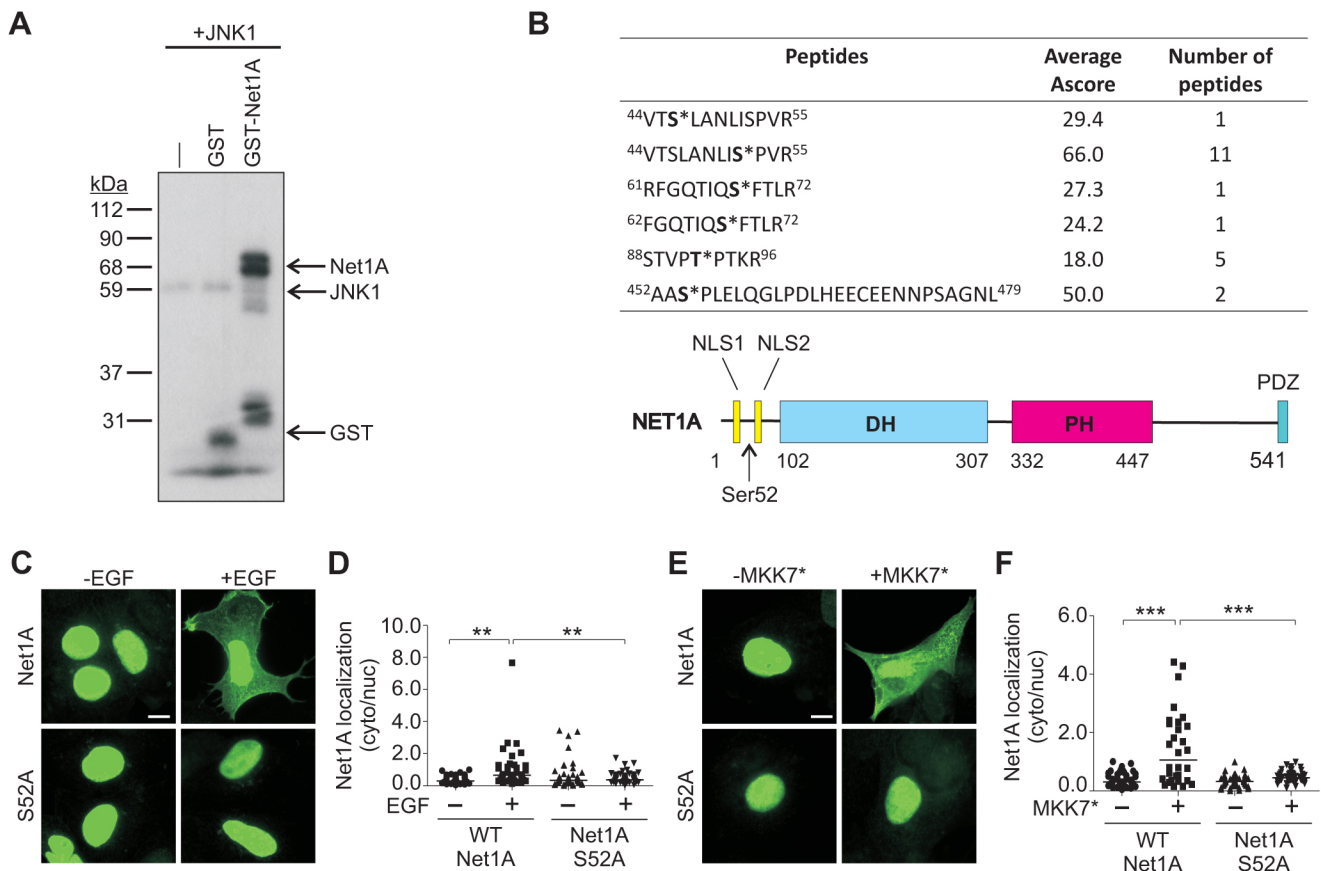


**Fig. 5. Identification of JNK1 phosphorylation sites in Net1A and their requirement for cytosolic localization.** (A) *In vitro* kinase assay using recombinant GST, GST-Net1A or no addition (–), with JNK1 and [ $\gamma$ -<sup>32</sup>P]-ATP. A representative autoradiograph from three independent experiments is shown. (B) Mass spectrometry analysis of Net1A phospho-peptides from an *in vitro* kinase assay using GST-Net1A and JNK1. Ascore values (ambiguity score) and the number of the times a given peptide was identified are shown. Phosphorylated residues are shown in bold with an asterisk. Shown below the table is a schematic of Net1A, including the position of serine 52. NLS, nuclear localization sequence; DH, Dbl homology; PH, pleckstrin homology; PDZ, binding site for PDZ domains. (C,D) MCF7 cells were transfected with wild-type (WT) HA-Net1A or HA-Net1A S52A, serum starved overnight and stimulated with EGF (15 min). Cells were fixed and stained for HA-Net1A. Representative images are shown. Data were obtained from three independent experiments. (E,F) MCF7 cells were transfected with the wild-type HA-Net1A or HA-Net1A S52A, with or without Flag-MKK7\*. Cells were serum starved overnight, fixed and stained for HA-Net1A. Representative images are shown. Data were obtained from three independent experiments. For all experiments at least 20 cells per condition were quantified. The line indicates the median values. \*\* $P$ <0.01; \*\*\* $P$ <0.001. Scale bars: 10  $\mu$ m.

To confirm that Net1A S52E stimulated GTP loading of RhoA, MCF7 cells were transfected  $\beta$ -Gal or Net1A constructs plus Flag-RhoA (Ozdamar et al., 2005), serum starved, lysed and tested for active RhoA by means of a pulldown assay with the GST-tagged Rho-binding domain (RBD) from rotoekin (O'Connor et al., 2000). We observed that Net1A S52E expression significantly stimulated GTP-loading of RhoA in these cells (Fig. 7F), consistent with its effects on MLC2 phosphorylation and F-actin accumulation. Thus, the elevated ability of Net1A S52E to stimulate RhoA signaling is primarily due to its enhanced cytosolic localization rather than an increase in its catalytic activity.

#### Cytosolic localization of Net1A stimulates cell motility and extracellular matrix invasion

Since RhoA activation contributes to multiple aspects of cell motility, we examined whether Net1A S52E expression stimulated motility in MCF7 cells. MCF7 cells are luminal subtype breast cancer cells that display an epithelial morphology and are far less motile than metastatic breast cancer cells. For these experiments, we transiently transfected cells by electroporation, which routinely resulted in transfection efficiencies of ~70% (not shown). After

electroporation, the cells were starved overnight, trypsinized and placed in a transwell apparatus with EGF as the chemotactic ligand. In these assays, we observed that wild-type Net1A overexpression stimulated a small increase in motility as compared to that seen upon nuclear  $\beta$ -Gal expression (Fig. 8A). This was expected, as exposure to EGF would be expected to enhance Net1A cytosolic localization in a transient manner. Importantly, expression of Net1A S52E, which we have shown to be constitutively localized to the cytoplasm, caused a much larger increase in cell motility (Fig. 8A). Expression of Net1A S52A was completely ineffective at stimulating MCF7 cell motility, as was expected due to its lack of cytosolic accumulation (Fig. 8A).

We then examined whether Net1A S52E expression caused MCF7 cells to become invasive by using Matrigel-coated transwells. MCF7 cells are non-metastatic and will not efficiently invade an extracellular matrix such as Matrigel. We observed that Net1A S52E expression caused a strong increase in invasion by these cells, which did not occur in  $\beta$ -Gal or Net1A S52A-transfected cells (Fig. 8B). Similar to what was seen in the motility assays, wild-type Net1A overexpression weakly stimulated Matrigel invasion (Fig. 8B).

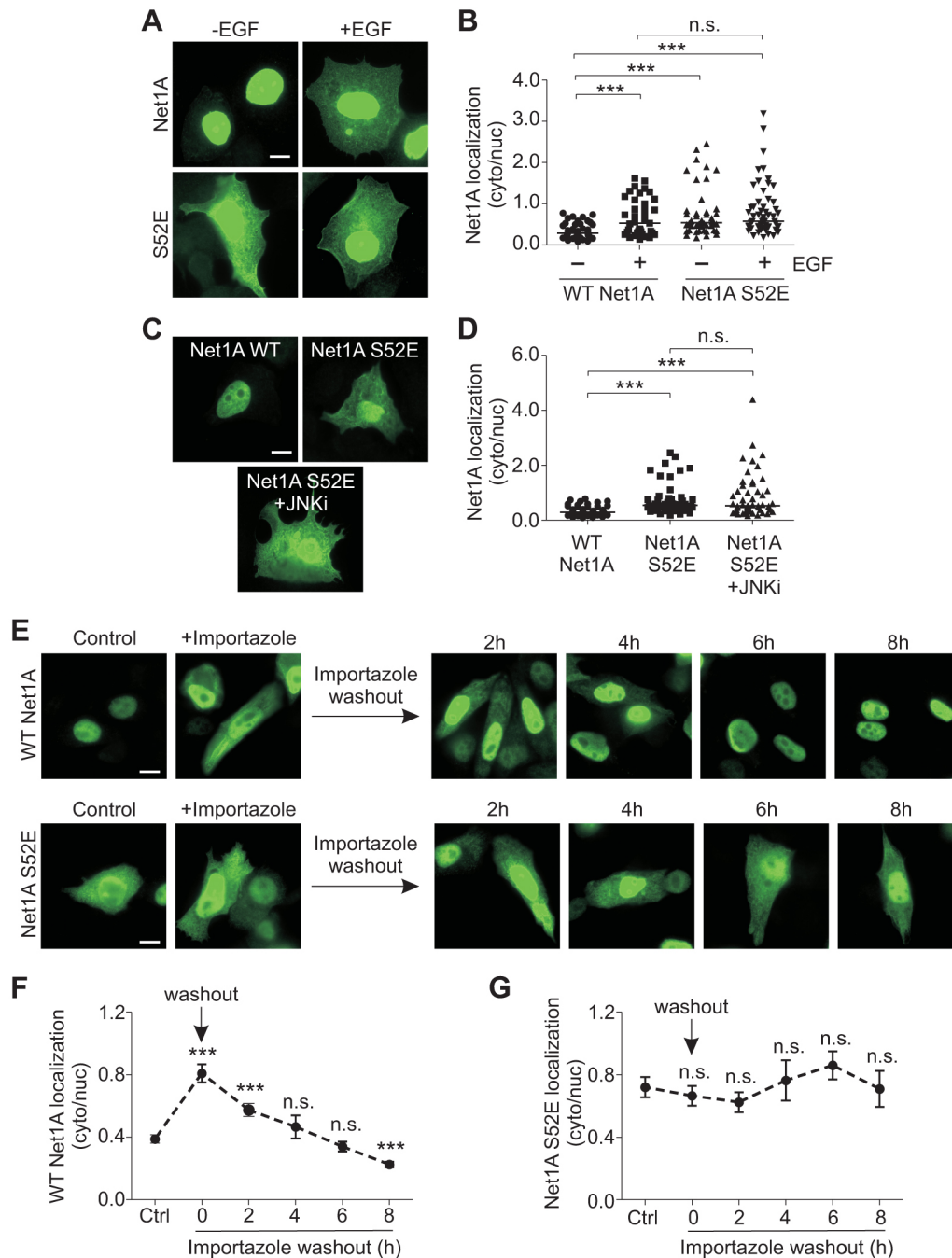


**Fig. 6. Substitution of a glutamate residue for serine 52 in Net1A results in cytosolic relocalization.** (A,B) MCF7 cells were transfected with wild-type (WT) HA–Net1A or HA–Net1A S52E, starved overnight, and stimulated with EGF for 15 min. Cells were then fixed and stained for HA–Net1A. Representative images are shown. Data were obtained from three independent experiments. (C,D) MCF7 cells were transfected with the wild-type HA–Net1A or HA–Net1A S52E, starved overnight and treated with the JNK inhibitor SP600125 (10  $\mu$ M; +JNKi) for 30 min. Cells were then fixed and stained for HA–Net1A. Representative images are shown. (E–G) MCF7 cells were transfected with wild-type HA–Net1A or HA–Net1A S52E, and starved overnight in the presence of importazole (40  $\mu$ M). The next day, importazole was washed out and cyclohexamide (50  $\mu$ g/ml), LMB (10  $\mu$ M) and MG132 (5  $\mu$ M) were added onto the cells. Cells were incubated for 0, 2, 4, 6 or 8 h, fixed and stained for HA–Net1A. Representative images are shown. Data were obtained from three independent experiments. For each experiment, at least 20 cells per condition were quantified. The line in B,D indicates the median values; results in F,G are mean $\pm$ s.e.m. \*\*\* $P$ <0.001; n.s., not significant. Scale bars: 10  $\mu$ m.

An early step in extracellular matrix invasion is the formation of invadopodia, which are transient filopodia-like protrusions that aid cells in degrading the surrounding extracellular matrix (Eckert and Yang, 2011; Parekh and Weaver, 2016). Importantly, wild-type Net1A overexpression has been recently shown to promote invadopodia formation in U2OS osteosarcoma cells (Schaffer

et al., 2015). To measure invadopodia formation, transfected MCF7 cells were plated overnight on coverslips coated with Oregon Green-conjugated gelatin, and then fixed and stained for HA–Net1A expression, F-actin, and DNA. Invadopodia were visualized as areas lacking Oregon Green fluorescence, and were quantified in terms of the number of invadopodia per cell, as well as

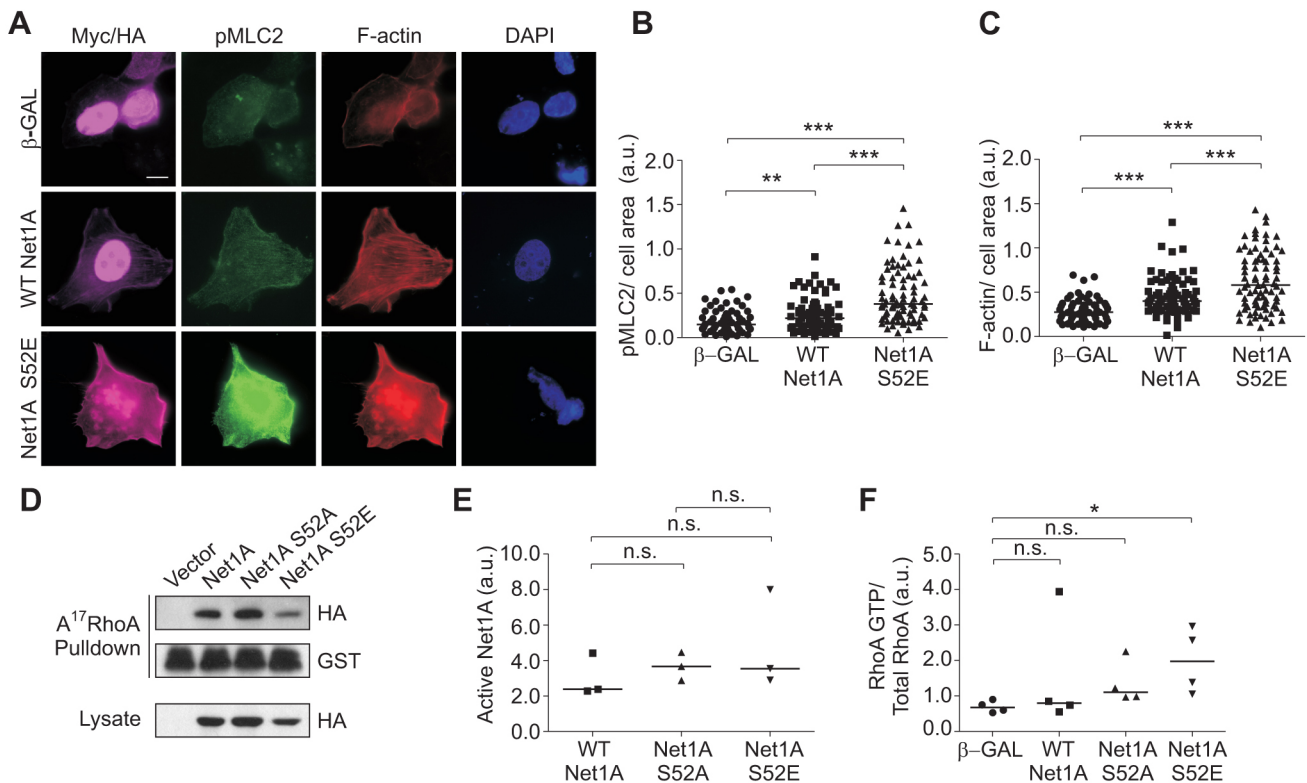


**Fig. 7. Net1A S52E expression stimulates RhoA signaling.** (A) MCF7 cells were transfected with wild-type (WT) HA–Net1A, HA–Net1A S52E, or Myc-tagged NLS– $\beta$ -galactosidase ( $\beta$ -GAL). Cells were then serum starved overnight, fixed and stained for phosphorylated (p)MLC2 (green), F-actin (red), DNA (blue) and the transfected proteins (magenta). Representative images are shown. (B,C) Quantification of pMLC2 (B) and F-actin levels (C). Data were obtained from three independent experiments. For each experiment, at least 20 cells per condition were quantified. (D) Net1A activity was assessed using GST–A<sup>17</sup>-RhoA pull-down assays. MCF7 cells were transfected with empty vector, wild-type HA–Net1A, HA–Net1A S52A and HA–Net1A S52E. At 2 days after transfection, cells were lysed and binding to GST–A<sup>17</sup>-RhoA was assessed by western blotting. Shown are representative blots from three independent experiments. (E) Quantification of GST–A<sup>17</sup>-RhoA pull-down results. Data are from three independent experiments. (F) RhoA activity was assessed using GST–RBD pull-down assays. Cells were transfected with Flag-tagged wild-type RhoA and the constructs shown. RhoA in the lysate and pull-down was detected by western blotting. Data are from three independent experiments. The line indicates the median values. \* $P$ <0.05; \*\* $P$ <0.01; \*\*\* $P$ <0.001; n.s., not significant. Scale bar: 10  $\mu$ m.

the mean gelatin degradation area per cell. Being non-invasive, MCF7 cells do not efficiently form invadopodia, and expression of  $\beta$ -Gal did alter this phenotype. On the other hand, wild-type Net1A overexpression caused cells to form a substantial number of invadopodia (Fig. 8C,E). However, these were invariably small, such that the area of gelatin degradation was not significantly different from that seen in  $\beta$ -Gal-transfected cells (Fig. 8F). On the other hand, Net1A S52E expression caused a strong increase in invadopodia number and degradation area compared to control cells (Fig. 8C–F). The presence of invadopodia in Net1A S52E-expressing cells was confirmed by confocal microscopy in cells co-stained for the invadopodia marker Tks5, which can be observed penetrating the fluorescent gelatin (Fig. 8D, xz plane). Invadopodia formation in cells expressing Net1A S52A was essentially the same as that in control cells (Fig. 8D–F). These data demonstrate that cytosolic localization of Net1A can cause breast cancer cells to become invasive, and that phosphorylation of Net1A on serine 52 is a key step in this process.

## DISCUSSION

We have shown previously that EGF stimulates Net1A cytosolic localization in a Rac1-dependent manner, and that this is necessary for Net1A-dependent RhoA activation and actin cytoskeletal rearrangement (Carr et al., 2013a,b; Song et al., 2015). However, it was unclear how Rac1 signaled to Net1A to cause its

relocalization. The work presented here indicates that activation of one or more MAPK pathways is required to stimulate Net1A cytosolic localization, and that activation of the JNK or p38 MAPK pathways is sufficient for this effect. These findings support a model in which EGF stimulation promotes CRM1-dependent nuclear export of Net1A, as well as JNK-dependent phosphorylation of Net1A on serine 52. Phosphorylation on serine 52 would prevent re-import of Net1A into the nucleus, thereby allowing for accumulation of Net1A in the cytosol. Extra-nuclear Net1A would then stimulate RhoA activation to support actomyosin contraction, cell motility and extracellular matrix invasion. Termination of Net1A signaling would be achieved by dephosphorylation of serine 52 and subsequent re-import into the nucleus, or by proteasomal-mediated degradation of Net1A (Carr et al., 2009, 2013b). Taken together, these data present a validated working model for how stress-activated MAPKs and CRM1 cooperate to allow ligand-stimulated cytosolic accumulation of Net1A and subsequent RhoA signaling.

Our work demonstrates that MEK1/2 and p38 MAPK inhibition, as well as JNK inhibition, can block EGF-stimulated Net1A cytosolic localization (Fig. 1). We focused on JNK-dependent regulation because Net1A localization was somewhat more sensitive to JNK inhibition. Moreover, Net1A $\Delta$ N overexpression has been shown previously to stimulate JNK signaling by interacting with the scaffolding protein CNK1 (also known as

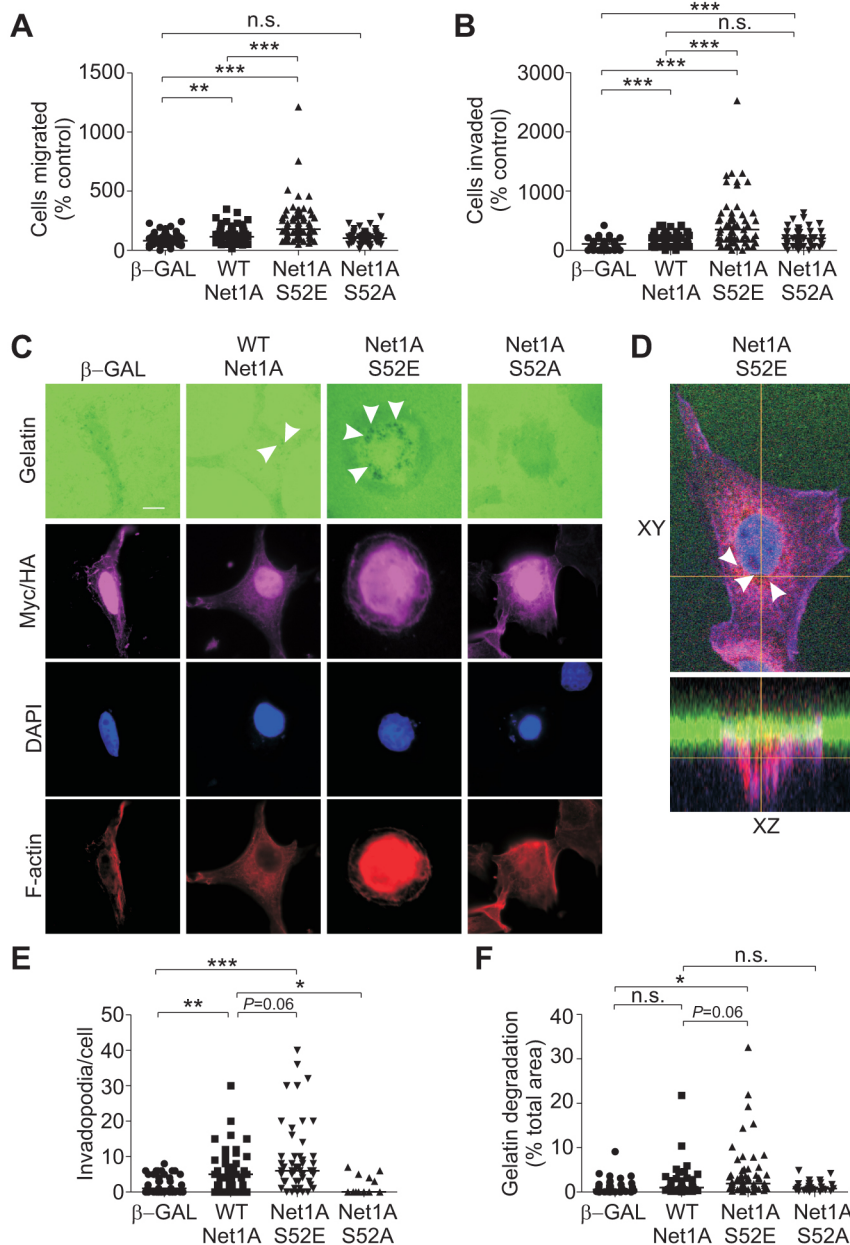


**Fig. 8. Net1A S52E expression stimulates cell migration, invasion and invadopodia formation.** (A,B) MCF7 cells were transfected with wild-type (WT) HA-Net1A, HA-Net1A S52E, HA-Net1A S52A or Myc-tagged NLS-β-galactosidase (β-GAL). Cells were serum starved and allowed to migrate towards EGF (100 ng/ml) in serum-free medium for 4 h (cell migration) or overnight (cell invasion). Data are from at least three independent experiments. (C) MCF7 cells were transfected with wild-type HA-Net1A, HA-Net1A S52E, HA-Net1A S52A or β-GAL. Cells were seeded on fluorescent gelatin (green)-coated coverslips and incubated in complete medium for 16–20 h. Cells were then fixed and stained for HA and Myc epitope tags (magenta), DNA (blue) and F-actin (red). Representative images are shown. (D) Representative confocal images showing xy and xz planes of a MCF7 cell expressing HA-Net1A S52E (purple) and seeded on fluorescent gelatin (green). Cells were also stained for Tks5 (red) and DAPI (blue). White arrowheads in C and D indicate invadopodia. (E) Quantification of the number of invadopodia per cell. (F) Quantification of degradation area per cell. For all experiments, at least 20 cells per condition were quantified. The line indicates the median values. \* $P < 0.05$ ; \*\* $P < 0.01$ ; \*\*\* $P < 0.001$ ;  $P = 0.06$  where indicated. Scale bar: 10  $\mu\text{m}$ .

CNKSR1) (Alberts and Treisman, 1998; Jaffe et al., 2004, 2005). Thus, Net1A appears to be connected to JNK signaling in multiple ways. However, our data also suggest that cytosolic accumulation of Net1A may be regulated by more than one MAPK. This may reflect the closely related substrate specificities of each MAPK family, as they are all proline-directed kinases. It may also indicate that relocalization of Net1A is a generalizable event that can be elicited by many ligands to stimulate RhoA activation. For example, we have observed previously that integrin ligation as well as stimulation with LPA potentially causes relocalization of Net1A to the cytosol. Moreover, this event is required for cell spreading after replating and for cell motility (Carr et al., 2013a,b; Murray et al., 2008). We have also shown here that TNF $\alpha$  stimulates Net1A relocalization in a JNK-dependent manner (Fig. 1), as does heregulin and FBS in invasive breast cancer cell lines (Fig. 3). In addition, others have noted that Net1A is required for actin cytoskeletal reorganization caused by TGF $\beta$  or cytolethal distending toxin (Guerra et al., 2008; Lee et al., 2010; Papadimitriou et al., 2012; Shen et al., 2001). Thus,

there is a growing list of stimuli that utilize Net1A to control RhoA signaling. Whether they require activation of one or more MAPK pathways for Net1A relocalization remains to be determined.

We have found that the activity of the nuclear exportin CRM1 is necessary for cytosolic localization of Net1A. Surprisingly, Net1A does not have a nuclear export signal (NES) sequence, suggesting that it must interact with another NES-containing protein to exit the nucleus. Previously it has been suggested that the PH domain of Net1 mediates its CRM1-dependent nuclear export, as fusion of the PH domain to the nuclear protein Rev drives cytosolic localization (Schmidt and Hall, 2002). Thus, we would expect that interaction with an NES-containing protein would require the PH domain of Net1A. The identity of such a protein, as well as the stimulus driving its association, remains to be determined.

Our data suggest that phosphorylation of serine 52 blocks nuclear re-import of Net1A, thus promoting Net1A cytosolic accumulation (Fig. 6E–G). The simplest interpretation of this result is that serine 52 phosphorylation creates a binding site for one or more proteins

that block access of nuclear importins to the N-terminal NLSs. Interestingly, serine 52 phosphorylation creates a predicted class IV WW domain binding site, which depends on a pS/pT-P motif (Eukaryotic Linear Motif Resource). Future work will be required to identify such proteins.

Although the stress-activated JNK and p38 MAPKs are most frequently associated with apoptotic and cytokine signaling, they have long been known to also control cell motility. This occurs through both transcription-dependent and -independent pathways (Huang et al., 2004; Xia and Karin, 2004). In the short term, acute inhibition of JNK and, to a lesser extent, p38 MAPK proteins, blocks cell motility in many cell types (Huang et al., 2004). Among the JNK substrates that are important for this effect are paxillin,  $\beta$ -catenin and the microtubule-associated proteins MAP1B and MAP2 (Chang et al., 2003; Huang et al., 2003; Kawauchi et al., 2003; Lee et al., 2009). There is also evidence that JNK plays a role in promoting breast cancer cell motility. For instance, treatment of MDA-MB-231 breast cancer cells with SP600125 blocks RANKL (also known as TNFSF11)-stimulated motility (Tang et al., 2011). JNK also suppresses EPS8 expression to enhance EGFR activation and breast tumor cell motility (Mittra et al., 2011). Moreover, DKK1-stimulated breast cancer metastasis to the lung requires JNK activation (Zhuang et al., 2017). Thus, our data suggests that regulation of Net1A localization and activity by stress-activated MAPKs represents an additional mechanism by which this family of kinases controls cell motility.

It is compelling that expression of Net1A S52E promotes cell motility and potently stimulates Matrigel invasion in MCF7 cells, which are normally weakly motile and non-invasive (Fig. 8A,B). These data support our previous observations that knockdown of Net1A in metastatic breast cancer cells inhibits their motility and invasion (Carr et al., 2013b), and suggest that cytosolic localization of Net1A is sufficient to drive cancer cell invasiveness. Consistent with these observations, Net1A S52E expression also potently stimulates invadopodia formation (Fig. 8C–F). Invadopodia are dynamic structures that require different mechanisms to initiate and mature. In this regard, RhoA has been shown to promote invadopodia maturation by stimulating ROCK-dependent actomyosin contraction, diaphanous-related formin-dependent F-actin polymerization and exocyst-dependent delivery of MT1-MMP (also known as MMP14) to invadopodia (Alexander et al., 2008; Lizarraga et al., 2009; Monteiro et al., 2013; Sakurai-Yageta et al., 2008). Thus, it is likely that cytosolic Net1A promotes invadopodia maturation in MCF7 cells, rather than stimulating their initiation. Exactly which aspects of invadopodia maturation are controlled by Net1A remains an open question. Interestingly, others have observed Net1A is phosphorylated on serine 46 by AMPK, and that mutation of this site to glutamic acid inhibits invadopodia formation caused by Net1A overexpression (Schaffer et al., 2015). As that group did not observe an effect of AMPK phosphorylation on the subcellular localization of Net1A, these findings suggest that serine 46 phosphorylation inhibits the ability of Net1A to signal to the invadopodia maturation machinery. It will be interesting in the future to assess the interplay between AMPK and JNK phosphorylation of Net1A in controlling invadopodia maturation and cell invasion.

## MATERIALS AND METHODS

### Cell lines and plasmids

MCF7 cells were as described in Song et al. (2015). BT-20, MDA-MB-436 and MDA-MB-453 breast cancer cells were a kind gift of Dr Jeffrey Chang, UT Houston Health Science Center, USA. All cell lines were confirmed to be mycoplasma free. MCF7, MDA-MB-436 and MDA-MB-453 cells were

cultured in Dulbecco's modified Eagle's medium (DMEM) with high glucose and glutamine (Hyclone) plus 10% (FBS) (Invitrogen), 100 U/ml penicillin and 100  $\mu$ g/ml streptomycin (HyClone). BT-20 cells were grown in DMEM/F12 supplemented as above. All cells were grown in 5% CO<sub>2</sub>, except for MCF7 cells, which were grown in 10% CO<sub>2</sub>. Cells were transfected using Lipofectamine Plus reagent (Life Technologies) according to the manufacturer's instructions. After transfection, cells were allowed to grow for an additional 48 h. For migration and invasion experiments, cells were electroporated in electroporation buffer with a Bio-Rad Gene Pulser XCell system. Cells were electroporated at a density of  $5 \times 10^6$  cells/pulse at 220 V/950  $\mu$ F (electroporation protocol obtained from Bio-Rad protocol library). Recombinant human epidermal growth factor (EGF) (R&D Systems) was used at 100 ng/ml. Recombinant human TNF $\alpha$  (R&D Systems) was used at 10 ng/ml concentration. Prior to treating the cells with EGF or TNF $\alpha$ , cells were starved overnight in DMEM plus 0.5% FBS and 1% penicillin-streptomycin. Inhibitors of JNK (SP600125; Selleck Chemicals), p38 MAPKs (SB202190; Selleck Chemicals) and MEKs (UO126; Calbiochem, Millipore) were dissolved in DMSO and cells were pretreated with the inhibitors at a 10  $\mu$ M concentration for 30 min before stimulation with EGF. The CRM1 inhibitor leptomycin B (LMB) was added at a concentration of 10  $\mu$ M and cells were incubated for 2 h or overnight.

Hemagglutinin (HA)-tagged mouse Net1A was as previously described (Carr et al., 2013a). pGEX-KG-Net1A was as described in Qin et al. (2005). Net1A S52A and S52E were generated by site-directed mutagenesis in pGEX-KG-Net1A and subcloned into pEF-HA cut with BamHI and EcoRI (New England Biolabs). Primers for site-directed mutagenesis were as follows: S52A-forward, 5'-TTGGCAAACCTAATCGCTCCCGTAAG-AAATGGA-3'; S52A-reverse, 5'-TCCATTCTTACGGGAGCGATTAA-GTTTGCCAA-3'; S52E-forward, 5'-TCTTTGGCAAACCTAATCG-AGCCCGTAAGAAATGGA-3'; S52E-reverse, 5'-TCCATTCTTACGG-GCTCGATTAAAGTTTGCCAAAGA-3'. Flag-tagged, constitutively active pcDNA3-MKK7 S198E/Thr202E (#14540) and pcDNA3-MKK3b S218E/T222E (#50449) were purchased from Addgene (Enslin et al., 2000; Lei et al., 2002). Myc-epitope tagged  $\beta$ -galactosidase with the NLS from SV40 Large T antigen and pGEX-2T-A<sup>17</sup>RhoA were as described previously (Song et al., 2015). Flag-tagged wild-type RhoA was as described previously (Ozdamar et al., 2005).

### Immunofluorescence and confocal microscopy

MCF7 cells were plated on acid-washed glass coverslips prior to transfection. For the immunofluorescence detection of proteins, cells on coverslips were fixed in 4% paraformaldehyde in PBS and permeabilized with 0.2% Triton X-100 in PBS plus 0.05% Tween 20 (PBST). Cells were incubated with the relevant primary antibodies diluted in PBST plus 1% BSA for 1 h at 37°C. After washing in PBST, cells were incubated for 30 min at 37°C with secondary antibodies diluted 1:1000 in PBST, plus 4', 6-diamidino-2-phenylindole (DAPI) (1  $\mu$ g/ml) (Sigma-Aldrich). Secondary antibodies were anti-mouse-IgG or anti-rabbit-IgG conjugated to Alexa Fluor 488, and anti-mouse-IgG or anti-rabbit-IgG conjugated to Alexa Fluor 594 (Life Technologies). For F-actin staining, Acti-stain 670-Phalloidin (Cytoskeleton) was used. Cells were then washed in PBST and coverslips were mounted on glass slides with Fluormount reagent (EMD Millipore Chemicals). Fluorescent staining was visualized using a Zeiss Axiophot epifluorescence microscope, and image acquisition was performed using Axiovision software. To evaluate Net1A localization, cytosolic-to-nuclear ratios of the fluorescence signals were calculated as previously described in detail (Song et al., 2015). Briefly, the intensity of fluorescent signal was quantified using ImageJ software (NIH) for HA-Net1A in the nuclear and cytosolic compartments. The nucleus was identified by DAPI staining and the cell area by F-actin staining. Background signals from each image were subtracted and the intensity of cytosolic over nuclear staining was quantified. For each experiment, a minimum of 20 cells were analyzed, and a minimum of three independent experiments were performed. Thus, quantification reflects a minimum of 60 cells per condition.

For the detection of the invadopodia marker Tks5, MCF7 cells were transfected with HA-Net1A S52E and, the next day, cells were counted and  $10^5$  cells were seeded onto fluorescent gelatin-coated coverslips, as described below. After 20 h, cells were fixed in 4% paraformaldehyde

and stained for Tks5, the HA tag and with DAPI. Cells were permeabilized with 0.1% Triton X-100 in PBS for 5 min and cells were incubated with primary and secondary antibodies with PBS washes in between. After mounting on slides with FluorSave reagent, confocal images were taken with a Nikon A1R confocal microscope. Z-stack images were acquired in 0.4  $\mu\text{m}$  steps with a 60 $\times$  objective lens. Images were visualized and analyzed with NIS Elements software. Antibodies used for immunofluorescence were as follows: mouse anti-HA tag (1:1000, sc-7392, Santa Cruz Biotechnology); mouse anti-Tks5 (1:100, sc-376211, Santa Cruz Biotechnology); rabbit anti-HA (1:1000, #3725, Cell Signaling); mouse anti-Myc epitope 9E10 (1:100, National Cell Culture Center); rabbit anti-pMLC2 (1:1000, #3671, Cell Signaling); mouse anti-Flag M2 (1:1000, F1804, Sigma).

### Western blot analyses

For western blotting, cells were washed with PBS and harvested in SDS lysis buffer (2.0% SDS, 20 mM Tris-HCl pH 8.0, 100 mM NaCl, 80 mM  $\beta$ -glycerophosphate, 1 mM  $\text{Na}_2\text{VO}_4$ , 20 mM NaF, 10  $\mu\text{g}/\text{ml}$  leupeptin, 10  $\mu\text{g}/\text{ml}$  pepstatin A, 10  $\mu\text{g}/\text{ml}$  aprotinin, 1 mM PMSF and 1 mM DTT). Harvested cells were sonicated and boiled for 5 min in the presence of Laemmli sample buffer. Equal volumes of cell lysates were resolved by SDS-PAGE. Proteins were transferred to polyvinylidene difluoride (PVDF) membranes and blocked in 5% non-fat dried milk in TBST for 1 h at room temperature. Membranes were incubated with the relevant antibodies diluted in TBST+0.05% milk, or 2% BSA, at 4°C overnight. Membranes were then incubated with horseradish peroxidase (HRP)-linked secondary antibodies, washed and immunoreactive bands were detected by ECL.

The specificity and efficacy of the MAPK inhibitors were confirmed by quantification of phosphorylation of the appropriate substrates for JNK, p38 MAPK, and MEK. The following antibodies were used: rabbit anti-p-c-Jun [pS63 (54B3), 1:250, #2361, Cell Signaling], rabbit anti-c-Jun (60A8, 1:1000, #9165, Cell Signaling), rabbit anti-pMK2 [pT334 (27B7), 1:1000, #3007, Cell Signaling], rabbit anti-MK2 (1:1000, #3042, Cell Signaling) mouse anti-pERK1/2 (pT202/pY204) (1:1000, #9106, Cell Signaling) and rabbit anti-ERK1/2 (1:1000, #4695, Cell Signaling). Western blots were quantified using ImageJ software.

### Kinetics of Net1A nuclear re-import

In order to determine the kinetics of Net1A nuclear re-import, cells were transfected with wild-type or S52E Net1A and serum starved in DMEM with 0.5% FBS. Importazole (40  $\mu\text{M}$ ) (Calbiochem-Millipore) was added overnight during the serum starvation. Cells were then washed three times with PBS to remove the importazole, replaced in starvation medium, and cycloheximide (50  $\mu\text{g}/\text{ml}$ ) (Sigma-Aldrich), LMB (10  $\mu\text{M}$ ) (LC Laboratories) and MG132 (5  $\mu\text{M}$ ) (Selleckchem) were added to stop protein synthesis, prevent nuclear export and block proteasome-mediated degradation, respectively. After incubation for different periods of time, cells were fixed with paraformaldehyde, processed for immunofluorescence microscopy, and Net1A localization was quantified as described above.

### Kinase assays and mass spectrometry

GST-Net1A was expressed in BL21DE3 *E. coli* and affinity purified using glutathione-agarose (Pierce), as previously described (Qin et al., 2005). *In vitro* kinase assays were performed with recombinant JNK1 purified from Sf9 cells (Signal Chem, M33). For kinase reactions, GST-Net1A (2  $\mu\text{g}$ ) was mixed with JNK1 (0.4  $\mu\text{g}$ ) and 2  $\mu\text{Ci}$  [ $\gamma$ - $^{32}\text{P}$ ]-ATP in kinase buffer (20 mM Tris-HCl pH 8.0, 2 mM  $\text{MgCl}_2$ , 1 mM DTT, 100  $\mu\text{M}$  ATP), and incubated for 15 min at 30°C. Reactions were terminated by the addition of Laemmli sample buffer. Samples were resolved by SDS-PAGE and the gels were stained with Coomassie Blue. Gels were then dried and exposed to X-ray film.

To identify phosphorylated peptides, the JNK1 and GST-Net1A kinase reaction was repeated without [ $\gamma$ - $^{32}\text{P}$ ]-ATP. The GST-Net1A band was excised from the Coomassie-stained gel and sent for mass spectrometry analysis (LC-MS/MS) to the Taplin Mass Spectrometry Facility (Harvard Medical School).

### GST-A<sup>17</sup>RhoA and GST-RBD pulldowns

GST-A<sup>17</sup>RhoA was expressed in BL21DE3 *E. coli* and purified using glutathione-agarose (Pierce), as described previously (Song et al., 2015).

For pulldown assays, two 10 cm plates of MCF7 cells were transfected with empty vector, or vectors for expression of HA-Net1A, HA-Net1A S52A or HA-Net1A S52E. Cells were washed with PBS and harvested in HEPES lysis buffer (20 mM HEPES pH 7.5, 150 mM NaCl, 5 mM  $\text{MgCl}_2$ , 1% Triton X-100, 1 mM DTT, 1 mM PMSF, and 10  $\mu\text{g}/\text{ml}$  each of aprotinin, leupeptin and pepstatin A). After 10 min incubation on ice, cells were centrifuged for 10 min at 16,100 g, 4°C. Equal amounts of the supernatant were incubated for 1 h at 4°C with 40  $\mu\text{g}$  GST-A<sup>17</sup>RhoA immobilized on glutathione-agarose. Proteins bound to GST-A<sup>17</sup>RhoA were precipitated by centrifugation and washed three times with the HEPES lysis buffer. After washing, beads were reconstituted in water plus 5 $\times$  Laemmli sample buffer and boiled for 5 min. Equal amounts of pulldown and input were resolved by SDS-PAGE, transferred to PVDF membranes, and processed for western blotting using rabbit anti-HA antibody (1:1000; 600-401-384, Rockland), to detect HA-Net1A, and a mouse anti-GST antibody (1:1000; sc-138, Santa Cruz Biotechnologies).

For the GST-RBD pulldown assays, cells were transfected with HA-Net1A constructs plus Flag-tagged wild-type RhoA and serum starved. Cells were then washed with PBS, trypsinized and pelleted by centrifugation (500 g, 5 min). Cell pellets were resuspended in 0.5% Triton lysis buffer plus 10 mM  $\text{MgCl}_2$  (0.5% Triton X-100, 10 mM  $\text{MgCl}_2$ , 20 mM Tris-HCl pH 8.0, 100 mM NaCl, 1 mM EDTA, 50 mM NaF, 80 mM  $\beta$ -glycerophosphate, 10 mM  $\text{MgCl}_2$ , 1 mM  $\text{Na}_2\text{VO}_3$ , 10  $\mu\text{g}/\text{ml}$  leupeptin, 10  $\mu\text{g}/\text{ml}$  pepstatin A, 10  $\mu\text{g}/\text{ml}$  aprotinin and 1 mM phenylmethylsulfonyl fluoride) and incubated on ice for 10 min. Insoluble material was removed by centrifugation (16,100 g, 10 min, 4°C) and lysates were incubated with 30  $\mu\text{g}$  of GST-RBD beads (Cytoskeleton, Inc.) for 1 h at 4°C. Beads were precipitated via centrifugation (16,100 g, 30 s, 4°C) and rinsed three times with wash buffer (25 mM Tris-HCl pH 7.5, 30 mM  $\text{MgCl}_2$ , 40 mM NaCl) to remove the unbound protein. Pellets were resuspended in 2 $\times$  Laemmli sample buffer and boiled for 5 min. Samples were resolved by SDS-PAGE, transferred to PVDF membranes, and processed for western blotting using mouse anti-Flag (1:1000, M2, F1804, Sigma) to detect Flag-RhoA, rabbit anti-HA antibody (1:1000; 600-401-384, Rockland) to detect HA-Net1A, and mouse anti-GST antibody (1:1000; sc-138; Santa Cruz Biotechnologies). Intensity of Flag-RhoA in the pulldown and lysate was quantified by densitometry.

### Cell motility, invasion and invadopodia assays

MCF7 cells were transfected with plasmids expressing Myc-epitope-tagged, NLS- $\beta$ -Gal, wild-type Net1A, Net1A S52E or Net1A S52A using electroporation. At 24 h after transfection, cells were trypsinized, counted with a hemacytometer and  $2.5 \times 10^5$  cells were seeded into the upper chambers of transwells containing 8- $\mu\text{m}$  pore membranes in 24-well plates (BD Biosciences). For cell invasion assays, 8- $\mu\text{m}$  pore membranes coated with Matrigel were used (BD Biosciences). The bottom chamber contained serum-free medium plus EGF (100 ng/ml). Cells were allowed to move towards the EGF for 4 h for migration and 16 h for invasion assays. At the end of the incubation period, cells in the upper chamber were removed with a cotton swab. Cells were then fixed in methanol and stained with DAPI (1  $\mu\text{g}/\text{ml}$ ). Ten images per membrane were obtained using a Zeiss Axiophot epifluorescence microscope and Axiovision software.

Gelatin degradation assays were performed to visualize invadopodia formation as described previously (Pichot et al., 2010) but with slight modifications. Briefly, acid-washed coverslips were precoated with 100  $\mu\text{g}/\text{ml}$  poly-L-lysine in a 24-well plate for 15 min followed by 0.5% glutaraldehyde fixation for 15 min at room temperature. Coverslips were coated with Oregon Green-labeled gelatin (Invitrogen, G-13186) on a warm block for 10 min and then treated with sodium borohydride (1 mg/ml) for 3 min at room temperature. After re-sterilizing the coverslips in 70% ethanol and quenching with serum-free DMEM,  $10^5$  cells were plated onto the coated coverslips and allowed to adhere for 20 h. The next day cells were fixed in 4% paraformaldehyde and stained for HA or Myc epitope tags, DNA (DAPI), and F-actin (Phalloidin-670). Invadopodia were counted from 8–10 random fields in each sample and the numbers averaged over at least three independent experiments. The area of degradation caused by invadopodia formation was determined with ImageJ as described previously (Martin et al., 2012). Briefly, for each cell, the gelatin degradation area was

calculated by thresholding the images with minimum pixel intensity values of  $38 \pm 7$  and  $46 \pm 7$  (mean  $\pm$  s.d.), and the area of matrix degradation was measured by using the 'analyze particles' window. The sum of all areas of degradation was divided by the cell area, as determined in the F-actin image.

### Statistical analysis

Comparisons among different treatment groups from western blot and immunofluorescence experiments were examined using unpaired Student's *t*-tests.  $P < 0.05$  was considered statistically significant. GraphPad Prism 5 software was employed for statistical analyses. All experiments were repeated at least three times. For immunofluorescence experiments at least 20 cells per condition per experiment were analyzed, and results from at least three separate experiments were combined.

### Acknowledgements

We thank members of the Cheng, Cunha, Denicourt, Dessauer, and Du laboratories for helpful discussions, and the Du laboratory for help with invadopodia experiments. We also thank Ilya Levental for help in quantifying invadopodia numbers and area using ImageJ.

### Competing interests

The authors declare no competing or financial interests.

### Author contributions

Conceptualization: A.U., J.A.F.; Methodology: J.A.F.; Investigation: A.U., W.O., Y.Z.; Resources: J.A.F.; Writing - original draft: A.U., J.A.F.; Writing - review & editing: A.U., J.A.F.; Supervision: J.A.F.; Project administration: J.A.F.; Funding acquisition: A.U., J.A.F.

### Funding

This work was supported by the National Cancer Institute (grant CA172129 to J.A.F.) and a postdoctoral fellowship from the Cancer Prevention Research Institute of Texas, UT Health Innovation in Cancer Prevention Research Training Program (RP160015 to A.U.). Deposited in PMC for release after 12 months.

### Supplementary information

Supplementary information available online at <http://jcs.biologists.org/lookup/doi/10.1242/jcs.204644.supplemental>

### References

- Alberts, A. S. and Treisman, R. (1998). Activation of RhoA and SAPK/JNK signalling pathways by the RhoA-specific exchange factor mNET1. *EMBO J.* **17**, 4075-4085.
- Alexander, N. R., Branch, K. M., Parekh, A., Clark, E. S., Iwueke, I. C., Guelcher, S. A. and Weaver, A. M. (2008). Extracellular matrix rigidity promotes invadopodia activity. *Curr. Biol.* **18**, 1295-1299.
- Beausoleil, S. A., Villén, J., Gerber, S. A., Rush, J. and Gygi, S. P. (2006). A probability-based approach for high-throughput protein phosphorylation analysis and site localization. *Nat. Biotechnol.* **24**, 1285-1292.
- Bennett, G., Sadlier, D., Doran, P. P., Macmathuna, P. and Murray, D. W. (2011). A functional and transcriptomic analysis of NET1 bioactivity in gastric cancer. *BMC. Cancer* **11**, 50.
- Bishop, A. L. and Hall, A. (2000). Rho GTPases and their effector proteins. *Biochem. J.* **348**, 241-255.
- Carr, H. S., Cai, C., Keinänen, K. and Frost, J. A. (2009). Interaction of the RhoA exchange factor Net1 with discs large homolog 1 protects it from proteasome-mediated degradation and potentiates Net1 activity. *J. Biol. Chem.* **284**, 24269-24280.
- Carr, H. S., Morris, C. A., Menon, S., Song, E. H. and Frost, J. A. (2013a). Rac1 controls the subcellular localization of the Rho guanine nucleotide exchange factor Net1A to regulate focal adhesion formation and cell spreading. *Mol. Cell. Biol.* **33**, 622-634.
- Carr, H. S., Zuo, Y., Oh, W. and Frost, J. A. (2013b). Regulation of focal adhesion kinase activation, breast cancer cell motility, and amoeboid invasion by the RhoA guanine nucleotide exchange factor Net1. *Mol. Cell. Biol.* **33**, 2773-2786.
- Chang, L., Jones, Y., Ellisman, M. H., Goldstein, L. S. B. and Karin, M. (2003). JNK1 is required for maintenance of neuronal microtubules and controls phosphorylation of microtubule-associated proteins. *Dev. Cell* **4**, 521-533.
- Cuadrado, A. and Nebreda, A. R. (2010). Mechanisms and functions of p38 MAPK signalling. *Biochem. J.* **429**, 403-417.
- Dutertre, M., Grataadou, L., Dardenne, E., Germann, S., Samaan, S., Lidereau, R., Driouch, K., de la Grange, P. and Auboeuf, D. (2010). Estrogen regulation and physiopathologic significance of alternative promoters in breast cancer. *Cancer Res.* **70**, 3760-3770.
- Ebelt, N. D., Cantrell, M. A. and Van Den Berg, C. L. (2013). c-Jun N-terminal kinases mediate a wide range of targets in the metastatic cascade. *Genes Cancer* **4**, 378-387.
- Eckert, M. A. and Yang, J. (2011). Targeting invadopodia to block breast cancer metastasis. *Oncotarget* **2**, 562-568.
- Enslin, H., Raingeaud, J. and Davis, R. J. (1998). Selective activation of p38 mitogen-activated protein (MAP) kinase isoforms by the MAP kinase kinases MKK3 and MKK6. *J. Biol. Chem.* **273**, 1741-1748.
- Enslin, H., Branch, D. M. and Davis, R. J. (2000). Molecular determinants that mediate selective activation of p38 MAP kinase isoforms. *EMBO J.* **19**, 1301-1311.
- Garcia-Mata, R., Dubash, A. D., Sharek, L., Carr, H. S., Frost, J. A. and Burridge, K. (2007). The nuclear RhoA exchange factor Net1 interacts with proteins of the Dlg family, affects their localization, and influences their tumor suppressor activity. *Mol. Cell. Biol.* **27**, 8683-8697.
- Gilcrease, M. Z., Kilpatrick, S. K., Woodward, W. A., Zhou, X., Nicolas, M. M., Corley, L. J., Fuller, G. N., Tucker, S. L., Diaz, L. K., Buchholz, T. A. et al. (2009). Coexpression of alpha6beta4 integrin and guanine nucleotide exchange factor Net1 identifies node-positive breast cancer patients at high risk for distant metastasis. *Cancer Epidemiol. Biomarkers Prev.* **18**, 80-86.
- Guerra, L., Carr, H. S., Richter-Dahlfors, A., Masucci, M. G., Thelestam, M., Frost, J. A. and Frisan, T. (2008). A bacterial cytotoxin identifies the RhoA exchange factor Net1 as a key effector in the response to DNA damage. *PLoS ONE* **3**, e2254.
- Heasman, S. J. and Ridley, A. J. (2008). Mammalian Rho GTPases: new insights into their functions in vivo studies. *Nat. Rev. Mol. Cell Biol.* **9**, 690-701.
- Holliday, D. L. and Speirs, V. (2011). Choosing the right cell line for breast cancer research. *Breast Cancer Res.* **13**, 215.
- Huang, C., Rajfur, Z., Borchers, C., Schaller, M. D. and Jacobson, K. (2003). JNK phosphorylates paxillin and regulates cell migration. *Nature* **424**, 219-223.
- Huang, C., Jacobson, K. and Schaller, M. D. (2004). MAP kinases and cell migration. *J. Cell Sci.* **117**, 4619-4628.
- Jaffe, A. B. and Hall, A. (2005). Rho GTPases: biochemistry and biology. *Annu. Rev. Cell Dev. Biol.* **21**, 247-269.
- Jaffe, A. B., Aspenstrom, P. and Hall, A. (2004). Human CNK1 acts as a scaffold protein, linking Rho and Ras signal transduction pathways. *Mol. Cell. Biol.* **24**, 1736-1746.
- Jaffe, A. B., Hall, A. and Schmidt, A. (2005). Association of CNK1 with Rho guanine nucleotide exchange factors controls signaling specificity downstream of Rho. *Curr. Biol.* **15**, 405-412.
- Johnstone, E. D., Mackova, M., Das, S., Payne, S. G., Lowen, B., Sibley, C. P., Chan, G. and Guilbert, L. J. (2005). Multiple anti-apoptotic pathways stimulated by EGF in cytotrophoblasts. *Placenta* **26**, 548-555.
- Kant, S., Swat, W., Zhang, S., Zhang, Z.-Y., Neel, B. G., Flavell, R. A. and Davis, R. J. (2011). TNF-stimulated MAP kinase activation mediated by a Rho family GTPase signaling pathway. *Genes Dev.* **25**, 2069-2078.
- Kawauchi, T., Chihama, K., Nabeshima, Y. and Hoshino, M. (2003). The in vivo roles of STEF/Tiam1, Rac1 and JNK in cortical neuronal migration. *EMBO J.* **22**, 4190-4201.
- Lee, M.-H., Koria, P., Qu, J. and Andreadis, S. T. (2009). JNK phosphorylates beta-catenin and regulates adherens junctions. *FASEB J.* **23**, 3874-3883.
- Lee, J., Moon, H.-J., Lee, J.-M. and Joo, C.-K. (2010). Smad3 regulates Rho signaling via NET1 in the transforming growth factor-beta-induced epithelial-mesenchymal transition of human retinal pigment epithelial cells. *J. Biol. Chem.* **285**, 26618-26627.
- Lei, K., Nimnual, A., Zong, W.-X., Kennedy, N. J., Flavell, R. A., Thompson, C. B., Bar-Sagi, D. and Davis, R. J. (2002). The Bax subfamily of Bcl2-related proteins is essential for apoptotic signal transduction by c-Jun NH(2)-terminal kinase. *Mol. Cell. Biol.* **22**, 4929-4942.
- Lizarraga, F., Poincloux, R., Romao, M., Montagnac, G., Le Dez, G., Bonne, I., Rigault, G., Raposo, G. and Chavrier, P. (2009). Diaphanous-related formins are required for invadopodia formation and invasion of breast tumor cells. *Cancer Res.* **69**, 2792-2800.
- Martin, K. H., Hayes, K. E., Walk, E. L., Ammer, A. G., Markwell, S. M. and Weed, S. A. (2012). Quantitative measurement of invadopodia-mediated extracellular matrix proteolysis in single and multicellular contexts. *J. Vis. Exp.*, **66**, e4119.
- Mitra, S., Lee, J.-S., Cantrell, M. and Van Den Berg, C. L. (2011). c-Jun N-terminal kinase 2 (JNK2) enhances cell migration through epidermal growth factor substrate 8 (EPS8). *J. Biol. Chem.* **286**, 15287-15297.
- Monteiro, P., Rossé, C., Castro-Castro, A., Irondele, M., Lagoutte, E., Paul-Gilloteaux, P., Desnos, C., Formstecher, E., Darchen, F., Perrais, D. et al. (2013). Endosomal WASH and exocyst complexes control exocytosis of MT1-MMP at invadopodia. *J. Cell Biol.* **203**, 1063-1079.
- Murray, D., Horgan, G., Macmathuna, P. and Doran, P. (2008). NET1-mediated RhoA activation facilitates lysophosphatidic acid-induced cell migration and invasion in gastric cancer. *Br. J. Cancer* **99**, 1322-1329.
- O'Connor, K. L., Nguyen, B.-K. and Mercurio, A. M. (2000). RhoA function in lamellae formation and migration is regulated by the alpha6beta4 integrin and cAMP metabolism. *J. Cell Biol.* **148**, 253-258.

- Ozdamar, B., Bose, R., Barrios-Rodiles, M., Wang, H. R., Zhang, Y. and Wrana, J. L. (2005). Regulation of the polarity protein Par6 by TGF $\beta$  receptors controls epithelial cell plasticity. *Science* **307**, 1603-1609.
- Papadimitriou, E., Vasilaki, E., Vorvis, C., Iliopoulos, D., Moustakas, A., Kardassis, D. and Stournaras, C. (2012). Differential regulation of the two RhoA-specific GEF isoforms Net1/Net1A by TGF- $\beta$  and miR-24: role in epithelial-to-mesenchymal transition. *Oncogene* **31**, 2862-2875.
- Parekh, A. and Weaver, A. M. (2016). Regulation of invadopodia by mechanical signaling. *Exp. Cell Res.* **343**, 89-95.
- Pichot, C. S., Arvanitis, C., Hartig, S. M., Jensen, S. A., Bechill, J., Marzouk, S., Yu, J., Frost, J. A. and Corey, S. J. (2010). Cdc42-interacting protein 4 promotes breast cancer cell invasion and formation of invadopodia through activation of N-WASp. *Cancer Res.* **70**, 8347-8356.
- Qin, H., Carr, H. S., Wu, X., Muallem, D., Tran, N. H. and Frost, J. A. (2005). Characterization of the biochemical and transforming properties of the neuroepithelial transforming protein 1. *J. Biol. Chem.* **280**, 7603-7613.
- Rae, J. M., Scheys, J. O., Clark, K. M., Chadwick, R. B., Kiefer, M. C. and Lippman, M. E. (2004). EGFR and EGFRvIII expression in primary breast cancer and cell lines. *Breast Cancer Res. Treat.* **87**, 87-95.
- Raman, M., Chen, W. and Cobb, M. H. (2007). Differential regulation and properties of MAPKs. *Oncogene* **26**, 3100-3112.
- Rossman, K. L., Der, C. J. and Sondek, J. (2005). GEF means go: turning on RHO GTPases with guanine nucleotide-exchange factors. *Nat. Rev. Mol. Cell Biol.* **6**, 167-180.
- Roulston, A., Reinhard, C., Amiri, P. and Williams, L. T. (1998). Early activation of c-Jun N-terminal kinase and p38 kinase regulate cell survival in response to tumor necrosis factor  $\alpha$ . *J. Biol. Chem.* **273**, 10232-10239.
- Sakurai-Yageta, M., Recchi, C., Le Dez, G., Sibarita, J.-B., Daviet, L., Camonis, J., D'Souza-Schorey, C. and Chavrier, P. (2008). The interaction of IQGAP1 with the exocyst complex is required for tumor cell invasion downstream of Cdc42 and RhoA. *J. Cell Biol.* **181**, 985-998.
- Schaeffer, H. J. and Weber, M. J. (1999). Mitogen-activated protein kinases: specific messages from ubiquitous messengers. *Mol. Cell. Biol.* **19**, 2435-2444.
- Schaffer, B. E., Levin, R. S., Hertz, N. T., Maures, T. J., Schoof, M. L., Hollstein, P. E., Benayoun, B. A., Banko, M. R., Shaw, R. J., Shokat, K. M. et al. (2015). Identification of AMPK phosphorylation sites reveals a network of proteins involved in cell invasion and facilitates large-scale substrate prediction. *Cell Metab.* **22**, 907-921.
- Schmidt, A. and Hall, A. (2002). The Rho exchange factor Net1 is regulated by nuclear sequestration. *J. Biol. Chem.* **277**, 14581-14588.
- Sever, R. and Brugge, J. S. (2015). Signal transduction in cancer. *Cold Spring Harb. Perspect. Med.* **5**, a006098.
- Shen, X., Li, J., Hu, P. P.-C., Waddell, D., Zhang, J. and Wang, X.-F. (2001). The activity of guanine exchange factor NET1 is essential for transforming growth factor- $\beta$ -mediated stress fiber formation. *J. Biol. Chem.* **276**, 15362-15368.
- Shen, S.-Q., Li, K., Zhu, N. and Nakao, A. (2008). Expression and clinical significance of NET-1 and PCNA in hepatocellular carcinoma. *Med. Oncol.* **25**, 341-345.
- Soderholm, J. F., Bird, S. L., Kalab, P., Sampathkumar, Y., Hasegawa, K., Uehara-Bingen, M., Weis, K. and Heald, R. (2011). Importazole, a small molecule inhibitor of the transport receptor importin- $\beta$ . *ACS Chem. Biol.* **6**, 700-708.
- Song, E. H., Oh, W., Ulu, A., Carr, H. S., Zuo, Y. and Frost, J. A. (2015). Acetylation of the RhoA GEF Net1A controls its subcellular localization and activity. *J. Cell Sci.* **128**, 913-922.
- Subik, K., Lee, J. F., Baxter, L., Strzepek, T., Costello, D., Crowley, P., Xing, L., Hung, M. C., Bonfiglio, T., Hicks, D. G. et al. (2010). The expression patterns of ER, PR, HER2, CK5/6, EGFR, Ki-67 and AR by immunohistochemical analysis in breast cancer cell lines. *Breast Cancer* **4**, 35-41.
- Tang, Z. N., Zhang, F., Tang, P., Qi, X. W. and Jiang, J. (2011). RANKL-induced migration of MDA-MB-231 human breast cancer cells via Src and MAPK activation. *Oncol. Rep.* **26**, 1243-1250.
- Tournier, C., Whitmarsh, A. J., Cavanagh, J., Barrett, T. and Davis, R. J. (1999). The MKK7 gene encodes a group of c-Jun NH2-terminal kinase kinases. *Mol. Cell. Biol.* **19**, 1569-1581.
- Tournier, C., Dong, C., Turner, T. K., Jones, S. N., Flavell, R. A. and Davis, R. J. (2001). MKK7 is an essential component of the JNK signal transduction pathway activated by proinflammatory cytokines. *Genes Dev.* **15**, 1419-1426.
- Tu, Y., Lu, J., Fu, J., Cao, Y., Fu, G., Kang, R., Tian, X. and Wang, B. (2010). Overexpression of neuroepithelial-transforming protein 1 confers poor prognosis of patients with gliomas. *Jpn. J. Clin. Oncol.* **40**, 388-394.
- Wagner, E. F. and Nebreda, R. (2009). Signal integration by JNK and p38 MAPK pathways in cancer development. *Nat. Rev. Cancer* **9**, 537-549.
- Weston, C. R. and Davis, R. J. (2007). The JNK signal transduction pathway. *Curr. Opin. Cell Biol.* **19**, 142-149.
- Xia, Y. and Karin, M. (2004). The control of cell motility and epithelial morphogenesis by Jun kinases. *Trends Cell Biol.* **14**, 94-101.
- Xia, Z., Dickens, M., Raingeaud, J., Davis, R. J. and Greenberg, M. E. (1995). Opposing effects of ERK and JNK-p38 MAP kinases on apoptosis. *Science* **270**, 1326-1331.
- Zhuang, X., Zhang, H., Li, X., Li, X., Cong, M., Peng, F., Yu, J., Zhang, X., Yang, Q. and Hu, G. (2017). Differential effects on lung and bone metastasis of breast cancer by Wnt signalling inhibitor DKK1. *Nat. Cell Biol.* **10**, 1274-1285.